The ASTRI-Horn Cherenkov camera: improvements on the hardware and software components

Giuseppe Sottile[a], Pierluca Sangiorgi[a], Carmerlo Gargano[a], Fabio Paolo Lo Gerfo[a], Mattia Corpora[a], Osvaldo Catalano[a], Milvia Capalbi[a], Teresa Mineo[a], Giovanni Contino[a], Benedetto Biondo[a], Giuseppe Leto[b], Salvatore Garozzo[b], Davide Marano[b], Alessandro Grillo[b], Fabio D'Anca[c], Vito Conforti[d], Fulvio Gianotti[d], Giovanni Pareschi[e], and Salvatore Scuderi[f] for the ASTRI Project http://www.astri.inaf.it/en/library/

[a]INAF/IASF Palermo, Via Ugo La Malfa 156, Palermo, Italy
[b]INAF/OA Catania, Via Santa Sofia 78, Catania, Italy
[c]INAF/OA Palermo, Piazza del Parlamento 1, Palermo, Italy
[d]INAF/OAS Bologna, Via Piero Gobetti 93/3, Bologna BO, Italy
[e]INAF/OA Brera, Via Brera 28, Milano MI, Italy
[f]INAF/IASF Milano, Via Alfonso Corti 12, Milano, Italy

ABSTRACT

ASTRI-Horn is an imaging atmospheric Cherenkov telescope developed by the Italian National Institute for Astrophysics (INAF), installed at the Serra La Nave Astronomical Station on Mount Etna (Italy). ASTRI-Horn detected the Crab proving the validity of its innovative camera and of the dual mirror configuration. Henceforth the telescope will play another important role. It will be the test bench for the upcoming cameras to be adopted for the ASTRI Mini-Array, a project led by INAF to build and operate an array of nine Cherenkov telescopes at the Observatorio del Teide (Tenerife, Spain). Moreover, the ASTRI-Horn camera will be used to test new technological solutions and explore innovative Cherenkov observation techniques. The Cherenkov camera uses Silicon-Photo Multiplier (SiPM) detectors. The fast front-end electronics implemented in the CITIROC ASIC is based on a custom peak-detector mode, which measures the electric pulses generated by the Cherenkov light flashes. The compact camera embeds all the components of a reliable thermal cooling system. This contribution gives a description of the upgrades of the ASTRI-Horn camera, which are the results of the lesson learnt during these years of sky observations. The improvements aim at correcting the drawbacks detected so far and at increasing the overall performance of the camera. The main ones are the increment of the power supplied to the photodetectors, the redesign of the Lids kinematic chain, a more efficient embedded calibration system, new control software routines and GUI.

Keywords: Cherenkov camera, Silicon Photomultiplier

1. INTRODUCTION

The ASTRI project, led by the Italian National Institute for Astrophysics (INAF), in the first phase was dedicated to the development and test of an end-to-end prototype of Imaging Atmospheric Cherenkov Telescopes (IACT), named ASTRI-Horn. This was characterized by innovative technological solutions: a dual mirror optical system based on a modified Schwarzschild-Couder design and a Cherenkov camera based on Silicon Photo-Multipliers (SiPM) with an innovative readout electronics.[1] ASTRI-Horn, located on Mount Etna, at the Serra La Nave Astronomical Station of the INAF Observatory of Catania(Italy),[2] has been successfully tested since 2014.[3] The science verification of the ASTRI-Horn telescope has been completed with the detection of the Crab Nebula in 2018.[4] After a period of testing and scientific observations, the Cherenkov Camera was subjected to maintenance in order to implement fixes and upgrades both in hardware and software, based on the experience gained during the verification and validation phases. After a description of the ASTRI-Horn camera, in this contribution

Giuseppe Sottile: E-mail: giuseppe.sottile@inaf.it, Telephone: (39) 091 6809 567

Advances in Optical and Mechanical Technologies for Telescopes and Instrumentation V,
edited by Ramón Navarro, Roland Geyl, Proc. of SPIE Vol. 12188, 1218830
 · 0277-786X · doi: 10.1117/12.2629634

we summarize the main upgrades implemented on each sub-system, describing the improvements that allow to increase the overall performances of the camera. Some upgrades have been designed in order to make the camera an efficient technological and scientific test bench for the future camera that will be used on the ASTRI Mini-Array,[5] that is being realized by the ASTRI collaboration. The array, composed by nine IACTs, is under construction at the Teide Astronomical Observatory, operated by the Instituto de Astrofisica de Canarias (IAC), in Tenerife (Canary Islands, Spain).

2. THE ASTRI CAMERA

The camera consist of 6 main subsystem: the Thermo-Mechanical Assembly, the Photon Detection Module, the Electronics, the Ancillary devices, the Harness and the Camera Server. The first five subsystems are embedded in the camera body, while the last one is located in the data center and communicates with the camera by an Ethernet link. All the subsystems, except the camera server, have been subject to fundamental improvements, as described in this work. Furthermore, also the software managing the camera has been subject to important upgrades. The ASTRI-Horn camera and its subsystems are described in detail in several documents[6,7] Anyway, it is useful to give here a summary of each subsystem of the camera and of the relevant main tasks.

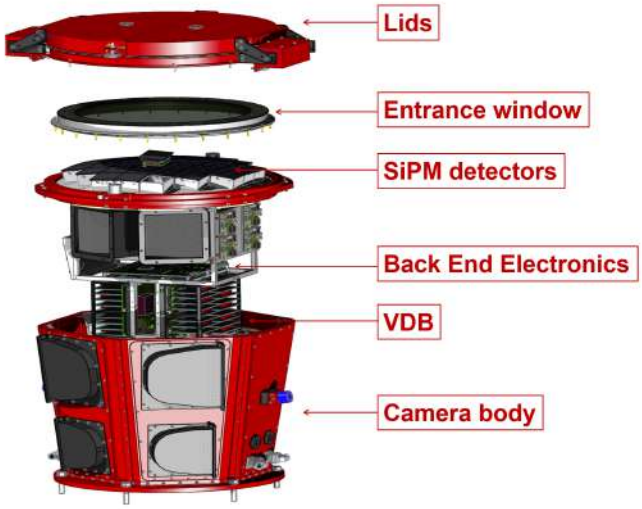

Figure 1. 3D model of the ASTRI Horn camera

2.1 Photon Detection Module

The Photon Detection Module is the assembly of the SiPM detectors tile, the Application Specific Integrated Circuit (ASIC) board, the Filed Programmable Gate Array (FPGA) board and the aluminum box, which contains and facilitate the heat dissipation from the three boards. Particularly, the metal box contributes to maintain a uniform temperature on the SiPM detectors. The SiPM tile is a single element composed by a matrix of 7mm x 7mm SiPM Hamamatsu detectors mounted on a printed circuit board (PCB) acting as a Cherenkov light sensor. At the moment of the procurement only 21 tiles were available and with two different technologies. 10 tiles were the LCT5-50um (Low Cross-Talk 5th Generation) and 11 tiles were LCT5-75um. The only difference between the two models is the dimensions of the microcells SPAD (single-photon avalanche photodiodes) composing the SiPM. The LCT5-50um contains 3600 SPADs of 50um and the LCT5-75um contains 2200 SPADs of 75um. The typical bias voltage for both models is in the range of 50-60 volts. Thus, the focal plane has been populated with only 21 PDM, though designed with 37 slots. The SiPM tile is connected with the ASIC Board, which hosts the two CITIROC[8] ASICs (Application Specific Integrated Circuit) and the two dual 12 bit ADCs AD7356 to digitally convert the analog outputs of the ASIC. In comparison with the other sampling Cherenkov camera, the innovation of the ASTRI one is the application of a Peak Detector per channel, designed specifically for INAF. This technical solution has several advantages, among them the smaller amount of data produced with

the detection and the lower power required. The ASIC board is connected from the bottom side with the FPGA board, which is based on the FPGA Xilinx 7 Artix-100 to manage all the PDM functions. Particularly, the FPGA firmware implements the topological trigger strategy, the communication with the two CITIROC and with the Back End Electronics (BEE) by a fast link differential SPI (Serial Peripheral Interface) for scientific data and by a UART for receiving commands. The board hosts also a few auxiliary chips and among them the power regulator/distributor (ADP5050), that generates the required low voltages for the correct working of the FPGA.

2.2 Back End Electronics

The heart of the ASTRI camera is the Back End Electronics (BEE), which controls and manages the overall camera behavior including the commanding of all the 37 PDMs, the data management, the lids mechanism control and the Calibration System, by means of a special FPGA with a System on Chip (SoC). The BEE receives commands from a remote Camera Control, arranges the packets containing the scientific and housekeeping data, and manages their transmission to a remote camera server. The link to the Camera Control and Camera Server is realized through two separate LANs. The BEE board hosts a commercial GPS for precise time stamping of the scientific events. The design of the BEE is based on a powerful FPGA of the family Xilinx Zynq, with a Linux Operating System running in its System-on-Chip (SoC) section. Therefore, the whole Camera Control is managed by an application software code running inside the Processing System of the Zynq. Other two FPGAs Xilinx Artix 7 200T located on the BEE are programmed with several firmware blocks and directly interfaced with all PDMs. The first one manages the interface with each PDMs, routing the messages sent from the Zynq and collecting all the answers. The communication between this FPGA and Zynq is performed by UART. The scientific data incoming from the PDMs follow a faster route to reach the Zynq. The second Artix7 hosts the second level trigger algorithm, receiving all the 37 first level trigger and providing the camera Trigger to all PDMs.

2.3 Voltage Distribution Box

The VDB is the sub-system of the ASTRI-Horn camera that is in charge of generating and distributing the operating voltages to the 37 PDMs. The VDB is composed by two identical mainboards (MB) and 37 daughterboards (DB). Each mainboard, which can host up to 19 daughterboards, receives the 24V input power and routes it to the installed boards. Each daughterboard generates all the required voltage rails for a PDM. This includes the low voltages to power the ASIC and the FPGA board and the high voltage (50V - 60V) to bias the SiPM photodetectors. All the voltages produced are switchable and programmable by the commands incoming from the Back End Electronics (BEE). In detail for each PDM the daughterboard provides:

- **High Voltage.** This is the voltage to bias the SiPM photodetectors. Generally, the bias voltage is the sum of two contributions: the breakdown voltage and the overvoltage, which span in the range of 2V and 3V, accordingly with the required gain charge.
- **FPGA.** This is the voltage required to power the FPGA Board, that can supply 4.5VDC-12 VDC. The maximum power required is 3W. The nominal voltage used in the ASTRI camera prototype is 4.6 VDC.
- **FEE_V1.** This is one of the 3 voltages required by the FEE-ASIC board to work. The maximum power required is 2W. The nominal voltage used in the ASTRI camera prototype is 3.6 VDC.
- **FEE_V2.** This is one of the 3 voltages required by the FEE-ASIC board to work. The maximum power required is 1W. The nominal voltage used in the ASTRI camera prototype is 5.4 VDC.
- **FEE_V3.** This is one of the 3 voltages required by the FEE-ASIC board to work. The output is programmable in the range -5.0 to -2.7 VDC. The maximum power required is 1W. The nominal voltage used in the ASTRI camera prototype is -3.3 VDC.

The BEE is connected to the first mainboard, identified as master, by a SPI serial bus. For this communication interface the BEE is the master, which provides the serial signal clock for each message exchanged to the

mainboard. The SPI is made over the LVDS electronic standard to increase the noise immunity of the bus. The mainboard master is connected to the second mainboard (the slave) by a RS485 serial link. The master mainboard receives the comands from the BEE, and redirects them to the second one. Each mainboard communicates with its own daughterboards by a multipoint RS485 network Fig.(2, 3, 4).

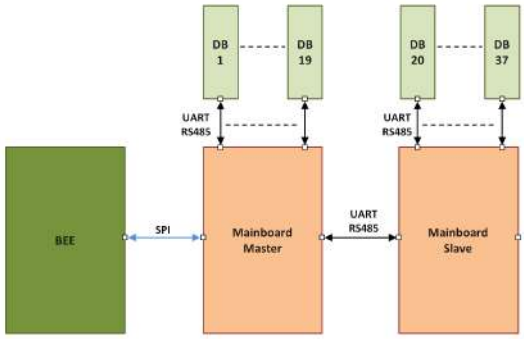

Figure 2. High level Block Diagram of the VDB. The Back End Electronics (BEE) send commands to the first mainboard, identified as Master, by the SPI (Serial Peripheral Interface). The communications among the VDB components (mainboards and daughterboards) are based on UART over a RS485 infrastructure. The two mainboards, Master and Slave, have the same hardware and differ only for the firmware.

Figure 3. mainboard PCB (dimensions 210mm x 150mm). In the centre of the board the NXP Kinetis microcontroller is placed, which manages the communications with the BEE, the daughterboards and the other mainboard. The picture on the right side shows the layer where the connectors are placed for the daughterboards insertion.

2.4 Calibration System

One of the ancillary devices equipping The ASTRI camera, the built in Calibration System performs the relative gain calibration of the SiPM photodetectors placed on the focal plane.[9] A side glow optical fiber, placed around the edge along the perimeter of the entrance window (Thermo-mechanical assembly), injects the light in the fused silica layers. The window scatters and diffuses the light of the fiber, lighting almost uniformly the focal plane. The source light of the system is the SLD3237VF blue laser diode (405nm) coupled to one of the end of the side glow fiber (fig.5). The blue laser diode is driven by the BEE through a Control Unit (PicoLAS PLCS-21) and a driver module (LDP-V 03-100 UF3), accordingly with the operative modes of the camera. The subsystem generates very short light pulses, up to 10ns, and a "pseudo-continuous" light, that are useful to emulate the Cherenkov flashes and the night sky background.

2.5 Thermo-mechanical Assembly

The Thermo-mechanical assembly is composed by several parts. Starting from the top to the bottom the main parts are the Lids, the entrance window, the Focal Plane Support Structure, the thermal control system, and the

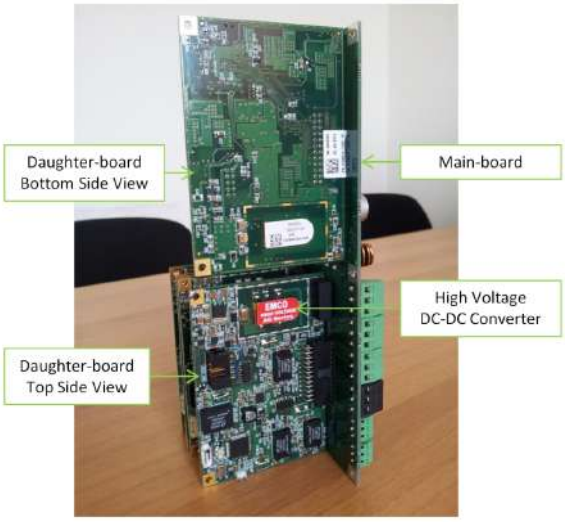

Figure 4. One of the mainboard with some of its daughterboards. The EMCO AG01 high voltage switching dc-dc regulator is visible on the daughterboard. In this case the AG01 is directly visible because the metal shielding cage was not installed.

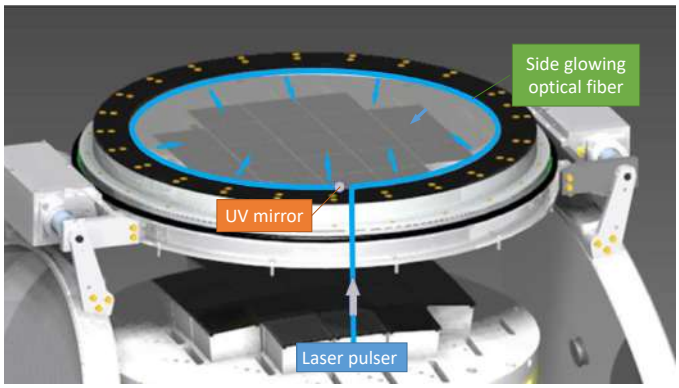

Figure 5. Operating principle of the camera calibration system

camera body. The Lids protect the entrance window from the external environment and guarantee the absolute darkness for the relative calibration of the camera on site. The entrance window, made by a stack of three layers of Fused Silica (Spectrosil), protects the SiPM photodetectors and avoids the thermal exchange with the external environment. The main function of the Spectrosil window is to increment the signal to noise ratio of the system, cutting-off a large portion of night sky background, since it acts as a IR-cut filter. The focal plane support structure (FPSS) is designed to equalize the temperature of the focal plane. It is made in aluminum, in which are embedded a net of heat pipes, capable to work even against gravity. The back of the FPSS is connected with the thermal regulation system, that is an assembly of a Peltier cell, other heat pipes and a fin stack. The embedded thermal regulation system is a very important characteristic of the ASTRI-Horn camera, and has shown a high reliability since the first tests on field.

3. ASTRI-HORN CAMERA UPGRADES

3.1 PDM

A problem of electrical noise was encountered and revealed during the staircase curve acquisition when the electronics stack was inserted in the metal box: because of a bad design of the FPGA board, the noise radiated from ADP5050 was picked up from the very sensitive inputs of the CITIROC. Initially the problem was solved

by applying a metal shield across the FPGA board to cover the converter. The drawback of this solution was the poor reliability of the system, that in some cases generated malfunctions, and the increased difficulty for the assembling. Another more reliable solution has been developed to shield the noise source from the sensitive receiver that consists in interposing two multilayers of shielding sheet between the boards stack(Fig.6). The first shield has been placed between the SiPM tile and the ASIC board (one layer of IFM10M-025BB300X200[10] and one layer of IFL16-030EB300X200[11]) and the second one between the ASIC and the FPGA board (two layer of IFM10M-025BB300X200 and two layer of IFL16-030EB300X200) .

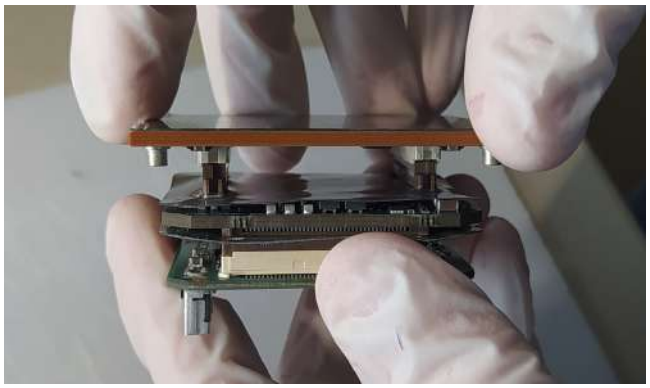

Figure 6. The shields placed respectively between the ASIC and the FPGA board and between the ASIC and the SiPM board

This solution shielded the CITIROC inputs from the ADP5050 noise source as shown in the figure 7.

3.2 VDB

Before 2020 the high voltage block was programmable in the range 50VDC to 60VDC at step of 150uV. The nominal maximum output current was 10mA. The daughterboard generated the high voltage using the EMCO AG01, a compact un-regulated DC-DC converter with its output isolated from the ground pin. Figure 8 shows the high voltage block diagram implemented in the daughterboard. Exposing the camera to the sky of Serra La Nave on Monte Etna, the VDB started to show some limits. The high Night Sky Background (NSB) of the Serra La Nave site combined with the high gain of SiPM saturated the current availability of the daughterboard high voltage section.[12] The consequence of the limited high voltage circuit performance was the reduction of the working duty cycle of the telescope. Another problem was discovered when the camera operated in Calibration Mode and in dark conditions (lids closed). Being the SiPMs current very low and consequently the EMCO lightly loaded, its output voltages grew far beyond its absolute maximum ratings damaging the system. This happened because the EMCO AG series are un-regulated converters, without a feedback network that could limit the output voltage escalation. The SiPMs detectors have not been at risk, because their bias voltage is provided by the linear regulator, which keeps the voltage constant independently of its input voltage. However, because of the high difference of voltage between input and output, the power dissipation of the linear regulator was inefficient, producing a rise in the temperature that compromised its performance.

The increment of the observation duty cycle drove the update of the high voltage section of the VDB. Initially, specific tests of the high voltage showed that the maximum current of 10mA was not sustained at the bias voltage of 55V set for the SiPMs. The main responsible of this limitation was the EMCO AG01, which overheated for high current values, close to 7mA – 8mA. The output high voltage started to go down, causing a decrease of the SiPM gain until they switched off. The daughterboard has been modified to improve its performance and to mitigate all these problems. The EMCO AG01 has been replaced by the more powerful and pin to pin compatible AGH01, which has a maximum output current of 15mA. To obtain all the current from the EMCO, a heat sink has been adopted, which is placed on the DC-DC converter, touching directly the metal plate under its enclosure (figure 9). The lab measurements showed that the absolute performance of the current provided to the SiPM detectors, in term of maximum load current and sustainability over the time, are doubled compared to the unmodified daughterboard (figure 10).

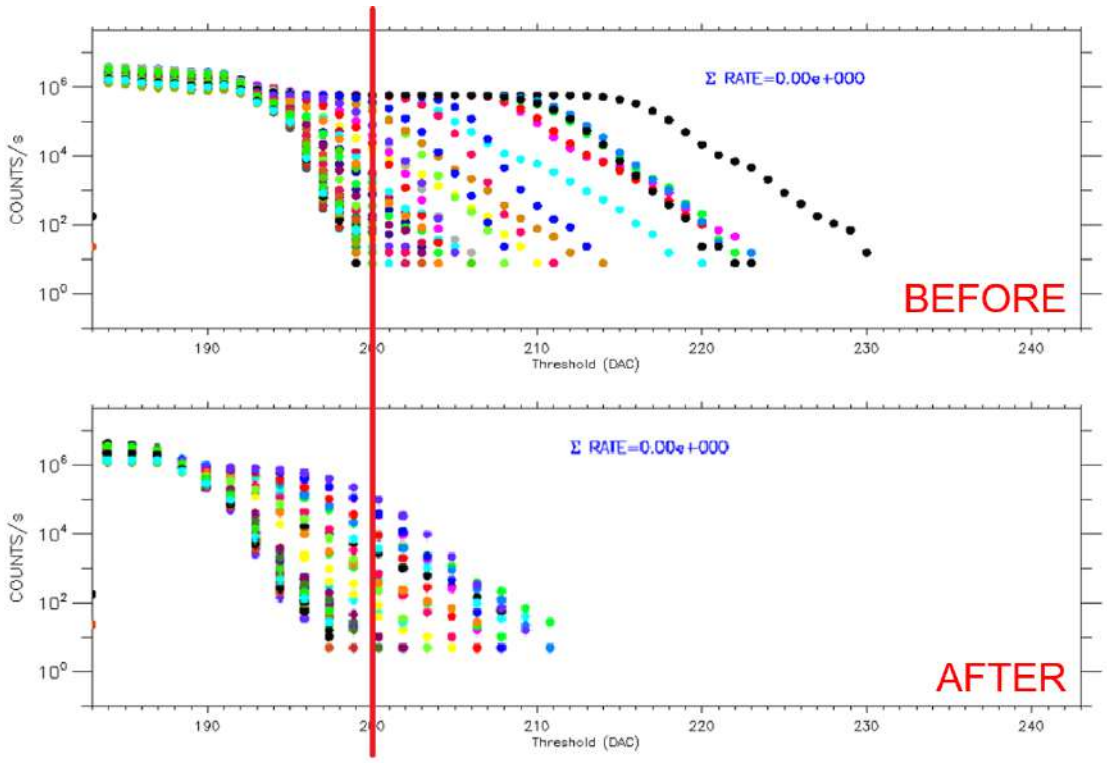

Figure 7.
Staircase curves for 64 pixel, captured while the high voltage needed to bias the SiPM is switched off. The upper graphs show the trigger counting without shielding sheets. The lower curves represent the trigger counts with shield sheets applied. In the latter case the trigger counting are smaller compared with the first one, demonstrating the effectiveness of the shielding.

The increased performances of the updated daughterboards have been verified after the installation on board of the camera. Although the current of the high voltage section cannot be directly measured (there isn't a current monitor on the daughterboard), thanks to the "Variance method" (VAR)[13] implemented on the ASTRI-Horn camera and to the Calibration Subsystem, it is possible to performs an indirect measurement. To this aim, we compute the Variance for increasing levels of continuous blue laser light of the Calibration Subsystem with Lids closed. Figure 11 reports the results obtained for all the PDM. When the laser is under-biased, the high voltage section provides a small quantity of current just sufficient to sustain the dark current. The current requirement of the SiPM increases with the light intensity of the laser and reaches a maximum beyond which the daughterboard can't provide it. As a consequence, for further increments of light intensity the current demand is so high that the high voltage section goes out of the load regulation range and is not capable to stabilize the output, so the high voltage decreases switching off the SiPM. An isolated feedback network has been applied to the EMCO, to limit the output overvoltage for very light load. A small PCB, populated by the feedback components, has been installed inside the metal cage to shield the AGH01. Another useful modification is the insertion of an electric load only during the switch on and off of the high voltage. In these phases, the high voltage should increase and decrease very slowly (order of seconds) following a linear ramp trend, to avoid any risk for the CITIROC ASICs. The load insertion permits a better control of the behavior of the voltage ramp. These modifications enhanced the reliability of the high voltage section.

3.3 Calibration System

After the first sky observing session, the Calibration System showed some drawbacks. Insufficient lights on the focal plane prevented the completion of the relative calibrations in a reasonable time, since the procedure had to be split into two steps involving PDM with different levels of illumination. Another problem was the insufficient

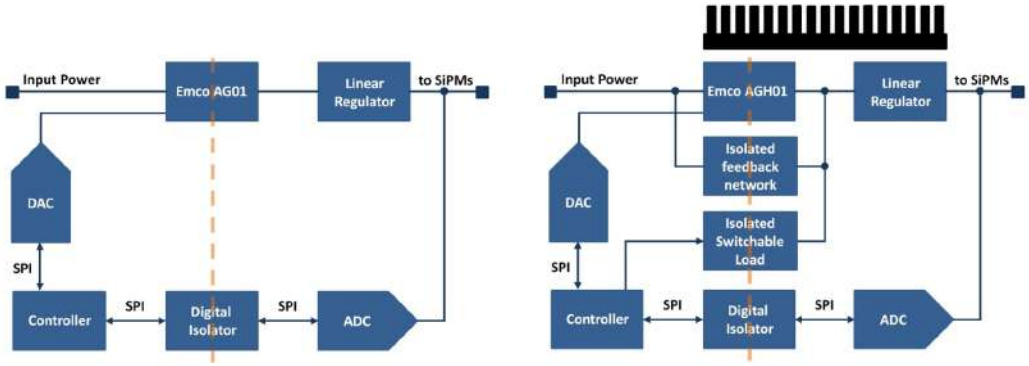

Figure 8. Block diagrams of the original daughterboard and of the improved one. The vertical dashed line indicates the separation between the digital and the isolated ground for the SiPM and the analog ASIC inputs. The higher complexity of the upgraded board corresponds to better a performances in terms of camera operation duty cycle and reliability. It is interesting to note that each afterwards added block has kept the ground separation as the original design.

Figure 9. Left: daughterboard with the AG01 high voltage DC-DC converter. Right: the improved daughterboard, populated by AGH01. It is evident the presence of the black heat-sink, that extracts the heat of the converter. The custom heat sink has a thermal contact with the high voltage linear regulator too, which decreases its temperature during the operations. A thermal interface glue has been used to simplify the installation. The new high voltage feedback network is not visible, because covered by the heat sink. The wire in the middle of the board is the digital line for the control of the switchable isolated load, which is used to facilitate the voltage management ramp. The daugherboard dimension are: 100mm x 70mm

reliability of the laser due to the generated heat, mainly exhibited during "pseudo-continuous" lighting, that required the replacement of the diode after some hours of work. The system has been inspected to remove these limitations and to increase its reliability. A new optical coupler and the polishing of the input fiber window allowed us to increase the intensity of the laser diode light inside the fiber. The output laser has been moved very close to the input end of the optical fiber, which has been lapped. At the end of the fiber, finished as the input one, a micro mirror (MIRO 4UV-C) has been attached, in order to increase the light intensity within the fiber. The hole for the diode accommodation perfectly matches with its TO18 package, making it easier to dissipate of the laser heat toward the large metal plate where the coupler is tightly screwed, and improving the reliability of the laser. (fig.12). The modifications of this sub-system allowed us to simplify the calibration procedures making them faster and more reliable.

3.4 Lids

A component of the Thermo-mechanical Assembly, the Lids of the ASTRI Horn camera is consist of two semi-circular metal doors, and protect the windows over the focal plane from dust and rain.[14] The system of gaskets, placed all around the circular perimeter of the window, and the magnetic-mechanical locking blocks guarantee

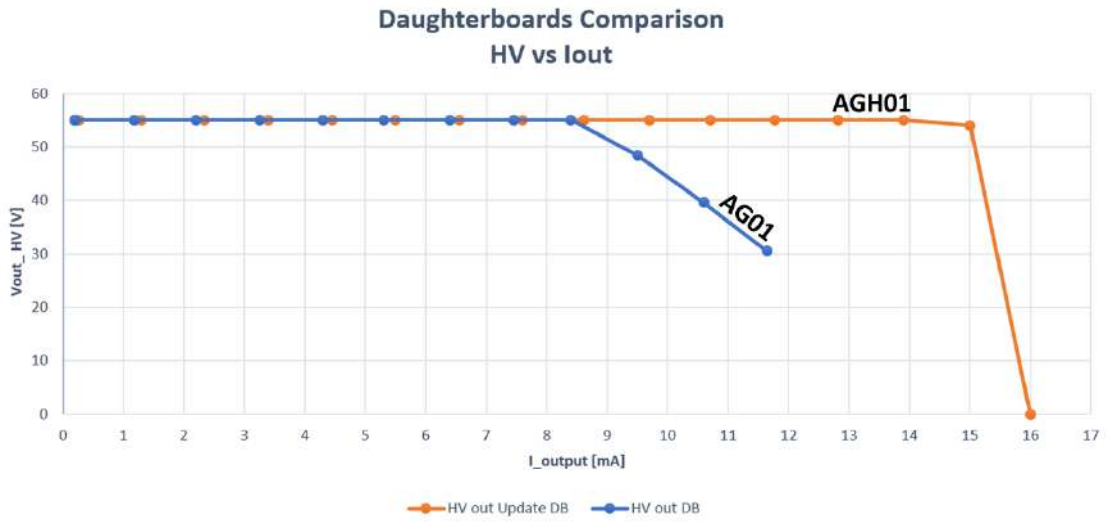

Figure 10. Comparison between the output currents of the daughterboard before and after the modifications. The updated daughterboard, equipped with the AGH01 provides more current than the one with the AG01 DC-DC converter. The current provided to the SiPM detectors is almost doubled, actually extending the observation time thanks the possibility to work with a higher level of NSB.

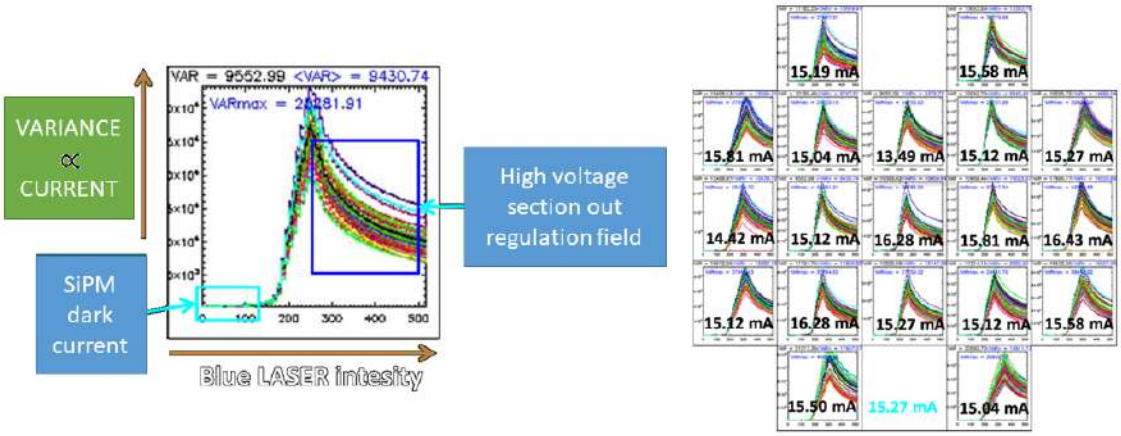

Figure 11. Left: the Variance measurement vs the intensity of the blue laser light intensity for each of 64 pixels the SiPM tile of the PDM. Right: variance measurements for the 21 PDM, populating the focal plane with the current maximum value provided by the corresponding daughterboard.

full darkness when the doors are in closed position. The full darkness provided by the Lids is critical especially during the calibration procedures, because the SiPM would detect the the light filtering through the seals so compromising the calibration of the focal plane. The doors motion is given by two stepper motors, each of which driven by a dedicated Nanotec SMCI12 controller and interfaced with the BEE. The movement of the motor shaft is stopped by the controller board, when the connected limit switch senses the presence of the door at its limit position. The locking of the Lids in the open and closed position is done by means of electro-permanent devices, which have a permanent magnetic field when not powered, while the magnetic field is switched off when the system is powered. This behavior is fundamental to hold the lids locked with the camera switched off or totally disconnected from the main power. The Nanotec SMCI12 controller receives the configuration parameters and commands from the BEE by a RS485 interface.[15] The Nanotec SMCI12 and the stepper motor are installed inside a small box, which is placed on the same plane of the windows as shown in figure 14. After some

Figure 12. The Picolas driver on board of the ASTRI-Horn camera. The aluminum block couples the laser with the fiber and allows the heat dissipation of the diode to the metal plate. On the right the figure shows the finishing of the optical fiber input after the lapping process.

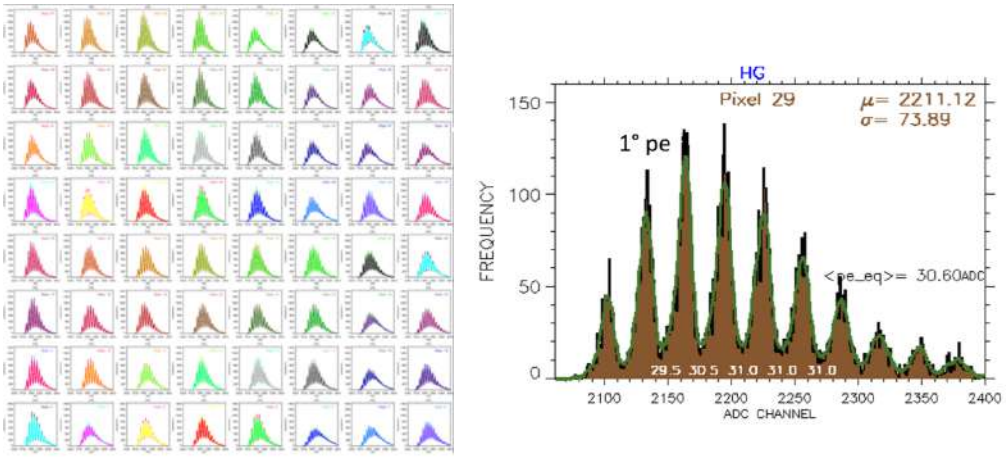

Figure 13. Left: the PHD of the 64 pixel of a SiPM tile that populate the focal plane, obtained by the Calibration System on board of the ASTRI-Horn camera. Right: the PDH of pixel 29. The plot shows the peak of the first pe_eq and reports the gains in terms of ADC unit for the first six photoelectrons equivalent. The mean pe_eq is 30.60 ADC unit.

observation campaigns the original design of the Lids assembly showed all its limit and drawbacks. The main problem was the automation of the doors that often stopped at wrong positions because of the bad locations of the limit switches. They were placed very close to the motor shaft providing the limit position with a very poor sensitivity. This was not the only drawback indeed they could send a wrong signals because of a relative skidding between the motor shaft, on which the reference metal plate was joint, and the door shaft. As a final result, the limit switches signaled the limit position reached by the reference plates but not the position of the doors. Finally, a problem of overheating of Nanotec controllers was observed, due to the narrow volume inside the boxes. To solve all these problems, the Lids design has been reviewed, beginning from the location of the limit switches and replacing the mechanical joints to avoid the skidding of the motor shaft. The new placements of the limit switches involved hardware modifications because they were incompatible with the operative modes of the Nanotec controllers, for which all software routines were well consolidated.

To make the new limit switches positions compatible with the "External Reference Run" mode used for the Nanotec controllers, an interface electronic board has been designed (figure 15). The board, named LAB (Limit switches adapter board) receives the limit switches signals and after some timing shifts provides them

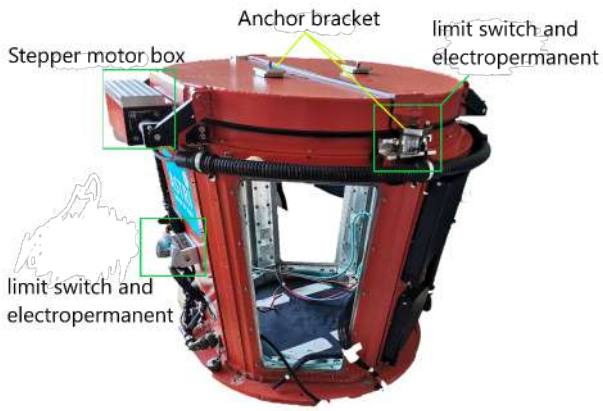

Figure 14. The camera body the components of the Lids sub-assembly. A corrugated black pipe protecting the cabling is also visible.

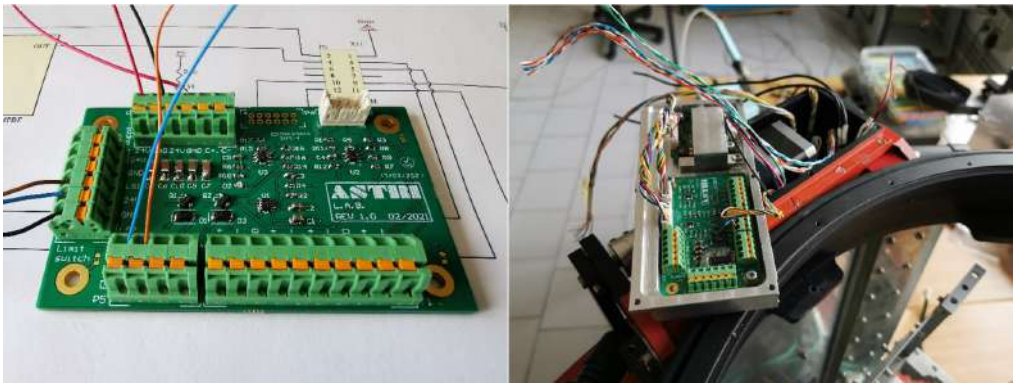

Figure 15. Left: the custom board LAB. Right: the Nanotec controller, which is partially hidden by the cold finger and the LAB installed on the aluminum cover.

to the inputs of the controllers. In addition, it hosts some power components that independently drive the electro-permanents avoiding the overheating of the controllers. Figure 16 shows the differences between the block diagrams after the modifications described here. The thermal aspect has been optimized replacing the covers of the boxes with others with a dedicated design and made of aluminum. The metal covers dissipate the heat of the controllers through cold fingers touching the power components. Finally, the design of the LAB better organizes the wiring inside the box, which had always been a weakness of the previous design.

3.5 Firmware and Software

During the camera upgrade program, several modifications on firmware and control software were also developed, both to support related modifications implemented on the hardware to control and to enhance the instrument with new features. Concerning the firmware we performed modifications oriented to enhance security and stability of fast data channel lines where data related to scientific events are sent from the PDMs to the BEE. To do that we added configurable masks on the lines related to the trigger signals and to the ADC values acquired from the readout electronics in order to enable the signal transmission only when strictly necessary according to the operational state of the camera. In this way, during configuration of the instrument or acquisition that not requires the use of that lines, they are disabled and the probability to be affected by noise is decreased. Another important feature in terms of firmware was the implementation of a complete broadcast communication between PDMs and BEE through the UART link devoted to the slow control. In the previous version of the firmware, the broadcast communication was implemented but its functionality was limited to the capability to dispatch the

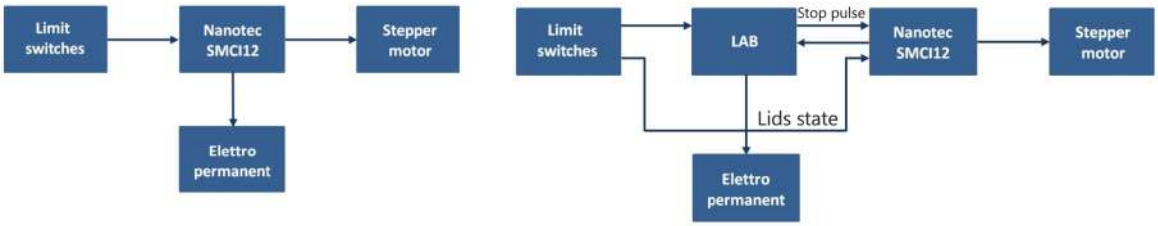

Figure 16. The block diagrams of the Lids control system before and after the modifications.

same message from the BEE to all the PDMs and receiving the response only from one of them. With this new complete implementation, the BEE is also able to collect each single response from each PDM, to check them by use of cyclic redundancy check and to produce a unique broadcast response with the composition of all the data received. This feature allows a boost in terms of velocity in communication especially during operations of data taking performed through the slow control, like the variance acquisition, resulting in the reduction of dead time. Just to quantify the difference between the procedure of data taking of variance data with single and broadcast communication, we pass from a communication of 42 messages (21 requests of 10 byte and 21 responses of 10962 byte) to only one request of 10 byte and one response of 10782 byte. In addition to the reduction of latency time due to performing 2 operations by software instead of 42, also the amount of data transmitted is reduced by 380 byte every acquisition (about every 2 seconds) because in the broadcast response composition procedure some fields like PDM ID, CRC, DATA LENGHT, etc are compressed. Compared to the last release of the software described in Sangiorgi[16] et al. (2019), upgrades concerning the control software involved both the camera control software deployed onboard the BEE to manage hardware and operating modes of the camera, and the Engineering GUI to control the instrument at high level. In the BEE camera Control software, in addition to the updated management of the hardware and the management of the new firmware features like the new message protocol structure for broadcast communication, we added new operating modes devoted to two new procedures for the instrument calibration. The first one is to determine the SiPM Breakdown Voltage, that consists of a series of variance data acquisitions at different values of bias voltage in a user specified range while the photodetectors are illuminated by a continuous light provided by the fiber optic calibration system. Data produced by this procedure, related to all PDMs at the different operating conditions, are stored in a structured file and allow to find the values of the breakdown voltage for all SiPMs and, consequently, the appropriate value of operating voltage for each PDM. The values of High Voltage thus determined will be provided to the PDMs by the corresponding daughterboard of the VDB. The second one is a particular automatized staircase curve procedure performed with 2 presets for the configuration of the CITIROC where the values of 4bit DAC fields are respectively set to the value 00 and FF. Data produced by this two acquisitions are acquired by the Data Acquisition server (DAQ) and allow to find, for each PDM, the proper values of the 4bit DAC fields of the CITIROC configuration in order to align the trigger thresholds among the 64 channels of the two different CITIROC installed in the same FEE board. At high level, the Engineering GUI was updated according to the philosophy to allow access, in addition to the management of a scientific observation, to particular operations by engineering and expert users, but enhancing the user experience in terms of friendly usage, access to information and data representation. To do this, the new main GUI integrates a large amount of acquired data representation in graphical form providing a quick look tool integrated in the control system (Fig. 17).

The new information graphically displayed is related to focal plane representation of variance data and Cherenkov images captured during observation. Since during an acquisition variance data are produced periodically in parallel independently of the current operating state of the camera, the user, through the variance image, can easily evaluate the conditions of the instrument and the observation context. For example, during the idle state the image can highlight bad pixels and electronic noise, while during calibration procedure the user can evaluate the level and uniformity of continuous light produced by the calibration system on the focal plane. Moreover, during the scientific observations, the user can monitor the NSB level and capture objects in the field of view like stars, meteors, debris or transient phenomena. In addition to the representation of the focal plane, light curves and distributions related to the whole focal plane or to each PDM or pixel are also available in a dedicated GUI (Fig. 18).

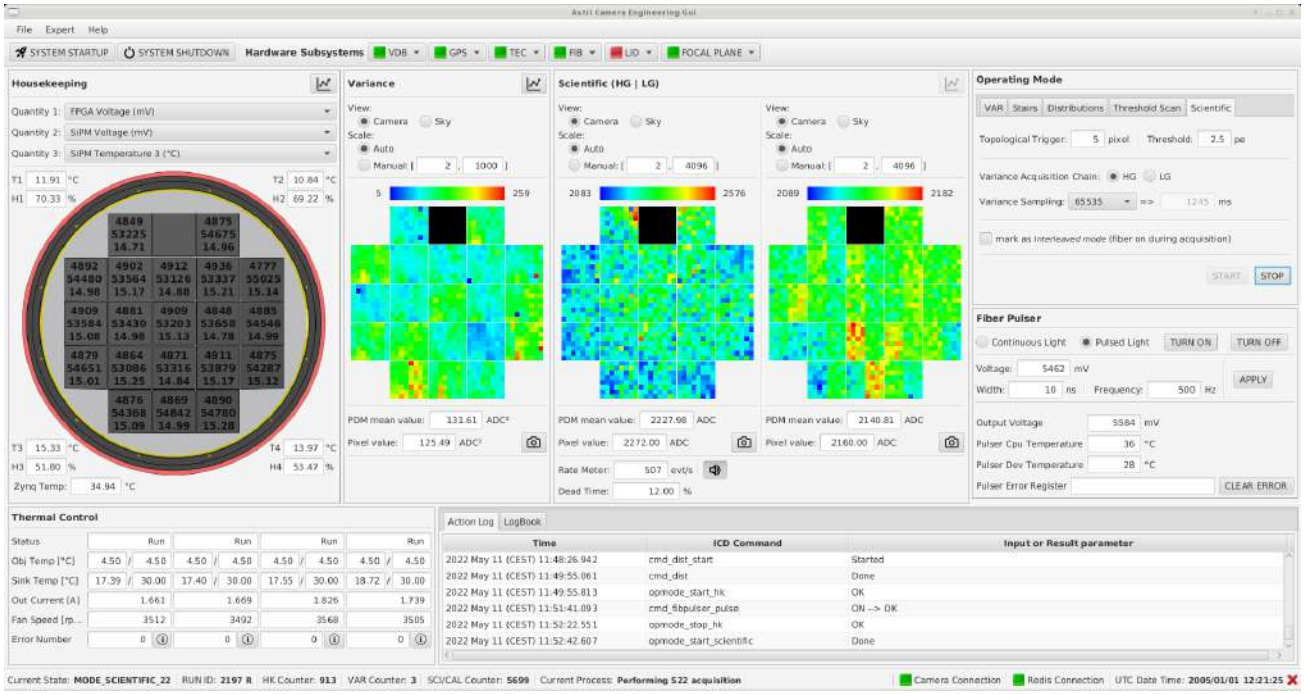

Figure 17. The Main Engineering GUI with HK, Variance and Scientific data quick look

Figure 18. Light curves and distribution of Variance data related to Focal plane, PDMs, Pixels

Cherenkov images are displayed for the two different acquisition chain of Low Gain and High Gain. Differently from housekeeping and variance, that are provided with a slow rate through the slow control between PDMs and BEE, this kind of data are not accessible directly from the control software of the BEE and from the GUI because dispatched directly to the DAQ. So, in order to provide this information to the user, the GUI displays only a sample of images (one per second) of the entire acquired data, retrieving them directly from the DAQ that was properly updated integrating a Redis server in order to provide this information to the GUI. Other operations like staircase procedure, in addition to the telemetry data supplied to the DAQ, provide the user with a real time representation of the data at the end of the process (Fig. 19). This allows the user to rapidly check the correct functioning of the instrument or highlight bad pixel behavior.

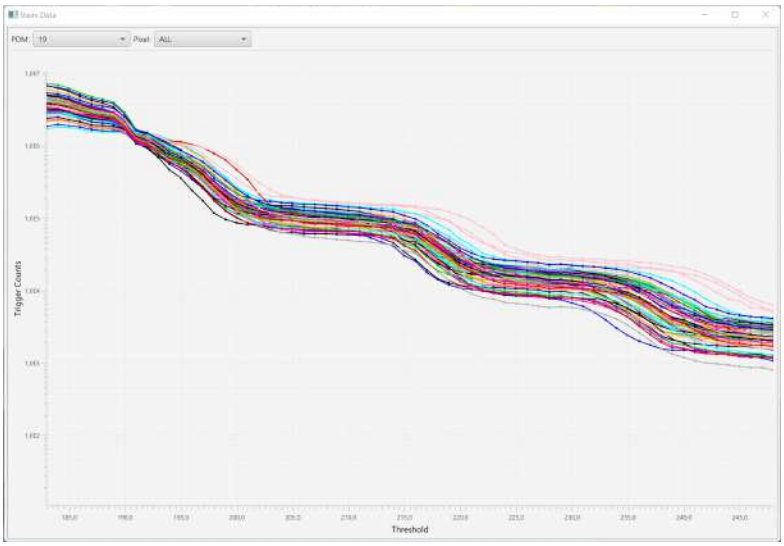

Figure 19. Staircase result plot

4. CONCLUSIONS

The aim of this paper is to describe the improvements of the ASTRI-Horn camera performed during the period between the end of 2019 and the end of 2021 while we all confronted with the Covid-19 pandemic. The camera has been installed on board of the ASTRI-Horn telescope at the end of 2021 in Serra La Nave on Mount Etna. During the winter of 2022 it has been constantly under test to verify all modifications applied while the environmental conditions were hostile. In spite for months the camera has been subject to rain, hail, snow, volcano dusts and low temperature, each subsystem has worked as expected. The modifications of the Lids solved the chronic problem of the past, and now worked as designed. Today, the increased VDB current capability permit the sky observation with higher value of NSB, in fact doubling the duty cycle of the camera. The Calibration System demonstrated the stability of the camera, since the parameters obtained on field are consistent with those obtained in lab. The firmware and software updates have speeded up the acquisition and interaction with the camera, making it more user-friendly. The modifications introduced in almost each subsystem will improve the quality of the observation and the use of the camera. Now the camera will be able to fulfill another important role as a test bench of the future ASTRI Mini-Array camera. The new algorithms developed for the array under construction (e.g. the trigger system), will be tested by the ASTRI-Horn camera in order to have a quick feedback.

ACKNOWLEDGMENTS

This work was conducted in the context of the ASTRI Project thanks to the support of the Italian Ministry of University and Research (MUR) as well as the Ministry for Economic Development (MISE) with funds specifically assigned to the Italian National Institute of Astrophysics (INAF). We acknowledge support from the Brazilian Funding Agency FAPESP (Grant 2013/10559-5) and from the South African Department of Science and Technology through Funding Agreement 0227/2014 for the South African Gamma-Ray Astronomy Programme. IAC is supported by the Spanish Ministry of Science and Innovation (MICIU). This work has also been partially supported by H2020-ASTERICS, a project funded by the European Commission Framework Programme Horizon 2020 Research and Innovation action under grant agreement n. 653477. The ASTRI project is becoming a reality thanks to Giovanni "Nanni" Bignami, Nicolo "Nichi" D'Amico two outstanding scientists who, in their capability of INAF Presidents, provided continuous support and invaluable guidance. While Nanni was instrumental to start the ASTRI telescope, Nichi transformed it into the Mini Array in Tenerife. Now the project is being built owing to the unfaltering support of Marco Tavani, the current INAF President. Paolo Vettolani and Filippo Zerbi, the past and current INAF Science Directors, as well as Massimo Cappi, the Coordinator of the High Energy branch of INAF, have been also very supportive to our work. We are very grateful to all of them. Nanni and Nichi, unfortunately, passed away but their vision is still guiding us. This article has gone through the internal ASTRI review process.

REFERENCES

[1] Sottile, G., Catalano, O., La Rosa, G., Capalbi, M., Gargano, C., Giarrusso, S., Impiombato, D., Russo, F., Sangiorgi, P., Segreto, A., et al., "ASTRI SST-2M camera electronics," in [*Ground-based and Airborne Telescopes VI*], **9906**, 99063D, International Society for Optics and Photonics (2016).

[2] Maccarone, M. C., Leto, G., Bruno, P., Fiorini, M., Grillo, A., Segreto, A., and Stringhetti, L., "The site of the ASTRI SST-2M telescope prototype," *Proceedings of the 33rd International Cosmic Rays Conference, ICRC 2013* **2013-October** (2013).

[3] Giro, E., Rodeghiero, G., Bonnoli, G., Canestrari, R., Conconi, P., Fiorini, M., Fantinel, D., Gardiol, D., Lessio, L., La Palombara, N., et al., "Tests characterization and alignment for the optics of the astri sst-2m telescope prototype for the cherenkov telescope array," in [*Advances in Optical and Mechanical Technologies for Telescopes and Instrumentation*], **9151**, 1176–1188, SPIE (2014).

[4] Lombardi, S., Catalano, O., Scuderi, S., Antonelli, L. A., Pareschi, G., Antolini, E., Arrabito, L., Bellassai, G., Bernlöhr, K., Bigongiari, C., et al., "First detection of the crab nebula at tev energies with a Cherenkov telescope in a dual-mirror Schwarzschild-Couder configuration: the ASTRI-Horn telescope," *Astronomy & Astrophysics* **634**, A22 (2020).

[5] Scuderi, S., Giuliani, A., Pareschi, G., Tosti, G., Catalano, O., Amato, E., Antonelli, L. A., Gonzàles, J., Bellassai, G., Bigongiari, C., Biondo, B., Boettcher, M., Bonanno, G., Bruno, P., Bulgarelli, A., Canestrari, R., Capalbi, M., Cardillo, M., Conforti, V., and Sanchez, R., "The astri mini-array of cherenkov telescopes at the observatorio del teide," *Journal of High Energy Astrophysics* (2022).

[6] Catalano, O., Giarrusso, S., Rosa, G. L., Maccarone, M. C., Mineo, T., Russo, F., Sottile, G., Impiombato, D., Bonanno, G., Belluso, M., Billotta, S., Grillo, A., Marano, D., Caprio, V. D., Fiorini, M., Stringhetti, L., Garozzo, S., and Romeo, G., "The astri sst-2m prototype: Camera and electronics," *Proceedings of the 33rd International Cosmic Rays Conference, ICRC 2013* **2013-October** (2013).

[7] Pareschi, G., "The ASTRI SST-2M prototype and mini-array for the Cherenkov telescope array (CTA)," in [*Ground-based and Airborne Telescopes VI*], **9906**, 99065T, International Society for Optics and Photonics (2016).

[8] Impiombato, D., Giarrusso, S., Mineo, T., Catalano, O., Gargano, C., La Rosa, G., Russo, F., Sottile, G., Billotta, S., Bonanno, G., et al., "Characterization and performance of the asic (citiroc) front-end of the ASTRI camera," *Nuclear Instruments and Methods in Physics Research Section A: Accelerators, Spectrometers, Detectors and Associated Equipment* **794**, 185–192 (2015).

[9] Impiombato, D., Catalano, O., Giarrusso, S., Mineo, T., Rosa, G. L., Gargano, C., Sangiorgi, P., Segreto, A., Sottile, G., Bonanno, G., et al., "Procedures for the relative calibration of the SiPM gain on ASTRI SST-2M camera," *Experimental Astronomy* **43**(1), 1–17 (2017).

[10] TDK, "IFM10M-025BB300X200 data sheet." Available online: https://product.tdk.com/system/files/dam/doc/product/noise_magnet-sheet/noise_magnet-sheet/noise-sheet-high/catalog/emc_noise-sheet_ifm_en.pdf.

[11] TDK, "IFM16-030EB300X200 data sheet." Available online: https://product.tdk.com/system/files/dam/doc/product/noise_magnet-sheet/noise_magnet-sheet/noise-sheet-high/catalog/emc_noise-sheet_ifm_en.pdf.

[12] Compagnino, A. A., Mineo, T., Maccarone, M. C., Catalano, O., Giarrusso, S., and Impiombato, D., "Evaluating the night sky background directly from the signal images detected by the ASTRI telescopes," *Experimental Astronomy* , 1–19 (2022).

[13] Segreto, A., Catalano, O., Maccarone, M. C., Mineo, T., La Barbera, A., and on behalf of the CTA ASTRI Project, F., "Calibration and monitoring of the ASTRI-Horn telescope by using the night-sky background measured by the photon-statistics ("variance") method," in [*Proceedings of 36th International Cosmic Ray Conference — PoS(ICRC2019)*], **358**, 791 (2019).

[14] Catalano, O., Capalbi, M., Gargano, C., Giarrusso, S., Impiombato, D., Rosa, G. L., Maccarone, M. C., Mineo, T., Russo, F., Sangiorgi, P., Segreto, A., Sottile, G., Biondo, B., Bonanno, G., Garozzo, S., Grillo, A., Marano, D., Romeo, G., Scuderi, S., Canestrari, R., Conconi, P., Giro, E., Pareschi, G., Sironi, G., Conforti, V., Gianotti, F., and Gimenes, R., "The ASTRI camera for the Cherenkov Telescope Array," in [*Ground-based and Airborne Instrumentation for Astronomy VII*], Evans, C. J., Simard, L., and Takami, H., eds., **10702**, 1038 – 1053, International Society for Optics and Photonics, SPIE (2018).

[15] Catalano, O., Maccarone, M. C., Gargano, C., La Rosa, G., Segreto, A., Sottile, G., De Caprio, V., Russo, F., Capalbi, M., Sangiorgi, P., et al., "The camera of the ASTRI SST-2M prototype for the Cherenkov telescope array," in [*Ground-based and Airborne Instrumentation for Astronomy V*], **9147**, 109–123, SPIE (2014).

[16] Sangiorgi, P., Capalbi, M., Catalano, O., Giarrusso, S., Gimenes, R., Impiombato, D., La Rosa, G., Russo, F., Segreto, A., Sottile, G., Grillo, A., Bonanno, G., Marano, D., Garozzo, S., Romeo, G., Conforti, V., Gianotti, F., and Trifoglio, M., "The ASTRI camera control software of the ASTRI SST-2M prototype for the Cherenkov telescope array," *Nuclear and Particle Physics Proceedings* **306-308**, 28–36 (2019). CRIS 2018 "Entering the Era of Multi-Messenger Astronomy".